Mercury-199 NMR of the Metal Receptor Site in MerR and Its Protein-DNA Complex

Lisa M. Utschig, James W. Bryson, Thomas V. O'Halloran*

Structural insights have been provided by mercury-199 nuclear magnetic resonance (NMR) into the metal receptor site of the MerR metalloregulatory protein alone and in a complex with the regulatory target, DNA. The one- and two-dimensional NMR data are consistent with a trigonal planar Hg-thiolate coordination environment consisting only of Cys side chains and resolve structural aspects of both metal ion recognition and the allosteric mechanism. These studies establish ^{199}Hg NMR techniques as useful probes of the metal coordination environment of regulatory proteins, copper enzymes, and zinc transcription factor complexes as large as 50 kilodaltons.

The chemical attributes of mercuric ion present unusual opportunities for study of biopolymer structure and function. Mercurials are *d*-block metal complexes that exhibit an extraordinarily high affinity for organic thiol-containing compounds known as mercaptans (literally, mercury seizing). Although mercurials are widely known protein-modifying agents that can inactivate some cysteine-containing enzymes or form heavy-metal derivatives with crystalline proteins, it is less well appreciated that mercuric ion binding does not always inactivate enzymes or disrupt protein structure (*1*). For instance, Hg(II) can be substituted for the native metal ion of several metalloenzymes in a manner that preserves catalytic activity. In the course of our attempts to understand the chemistry of Hg(II) in biological environments, we have focused on the mercuric ion receptor MerR, a protein that senses changes in the intracellular metal ion concentration and activates transcription of the genes responsible for Hg(II) detoxification. In this article we apply homonuclear and heteronuclear ^{199}Hg NMR methods to delineate the metal ion receptor environment of MerR and to provide insights into the allostery of MerR-DNA interactions. We show that Hg(II) can be substituted into a wide range of copper and zinc metalloproteins and demonstrate that the native coordination environments are readily determined by a combination of ^{199}Hg NMR methods. These results reveal several unexpected advantages relative to ^{113}Cd NMR in structure-function studies of relatively large metalloproteins.

The spin-1/2 ^{199}Hg isotope exhibits several favorable NMR properties for structural and functional studies, including a natural abundance of 16.8%, a receptivity 5.4 times that of ^{13}C, large coupling constants (*2*), and a chemical shift range of more than 5000 parts per million (ppm) (*3*); however, methods based on it have found limited application in probing the metal coordination environment in biologically relevant complexes (*4*, *5*) and metalloproteins (*2*, *6*, *7*).

The MerR metalloregulatory protein acts as a selective and sensitive metal ion sensor that activates expression of the stress responsive mercury detoxification (*mer*) genes (*8*). MerR responds to nanomolar Hg(II) concentrations and can stimulate transcription at this threshold even in the presence of a 10^6-fold excess of competing Hg(II) ligands, such as the mercaptan dithiothreitol (*9*). MerR is also selective and discriminates against gratuitous inducers such as Zn(II), Cd(II), Ag(I), and Au(I) that otherwise exhibit chemical similarities to Hg(II) (*9*).

This regulatory protein binds Hg(II) specifically and with high affinity. Subsequently it does work on the DNA. In the absence of Hg(II), MerR binds tightly to DNA and represses transcription. Metal binding to the protein/DNA complex stimulates transcription by inducing changes in the conformation of the DNA, making the promoter a better template for the enzyme RNA polymerase (RNAP) (*10*, *11*).

Establishing the allosteric mechanism and the molecular basis of metal ion recognition in this heterotropic receptor requires insights into the effect of MerR/DNA interaction on the structure of the metal binding site. Because the protein must alter the DNA structure in the metal-induced activation event, the final metal coordination environment may differ in the presence or absence of the DNA. Physical-inorganic (*12*), extended x-ray absorption fine structure (EXAFS) (*13*), and mutagenesis (*14*, *15*) studies have implicated the coordination of at least three Cys side chains to Hg(II) in the metal ion receptor site of MerR when it is not bound to the DNA. The presence of other ligands in the Hg(II) coordination environment, such as His and Met, have not been addressed by direct methods. Given that other structurally characterized Hg proteins exhibit higher coordination numbers, this aspect of the metal recognition problem remains in question.

Multidimensional NMR approaches to the three-dimensional (3D) structure of this metalloprotein are not feasible given the low solubility of the native protein (0.5 mM), the large size of the MerR dimer (32 kD), and the asymmetry of the stoichiometric complex [one Hg(II) per dimer] (*8*). Such limitations to physical probes are not unique to the Hg-MerR system. The need for structural insights about local metal coordination environments is underscored by the recent discoveries of new classes of putative metal binding motifs in enzymes, transcription factors, and regulatory proteins (*16*–*18*). After further establishing relations between structures and ^{199}Hg chemical shifts for an array of model complexes and Hg-substituted metalloproteins presented here, we conclude that the primary Hg(II) coordination environment is Hg(S-Cys)$_3$ and remains unchanged when MerR binds to its regulatory target DNA. This work further demonstrates that 1D and 2D ^{199}Hg NMR methods can establish the identity and number of several types of ligated side chains in Zn, Cu, and Fe biopolymer complexes as large as 50 kD.

Metal-proton chemical shift correlation in large proteins. Two-dimensional chemical-shift correlation methods allow direct detection of protons coupled to a heteronucleus. Heteronuclear multiple quantum coherence (HMQC) experiments have provided independent identification of Cys (*19*–*21*), His, and Met (*22*) as Cd(II) ligands in several ^{113}Cd-substituted proteins (*23*). This method has the potential to reveal similar interactions in MerR (a 288–amino acid dimer). Unfortunately, neither ^{1}H{^{113}Cd} or ^{1}H{^{199}Hg} HMQC experiments have been reported on proteins larger than 100 amino acids (*23*). Attempts to observe ^{1}H{^{113}Cd} HMQC spectra for ^{113}Cd-substituted MerR, by using delays established in successful ^{113}Cd-substituted plastocyanin experiments, yielded no signal (*24*).

^{1}H{^{199}Hg} HMQC studies of a structurally characterized protein. Given concerns about the contributions of chemical shift anisotropy (CSA) to ^{199}Hg linewidths and relaxation times for complexes with low coordination numbers (*4*), we optimized acquisition parameters for the ^{1}H{^{199}Hg} HMQC detection of Cys, Met, and His protons on the ^{199}Hg form of a

The authors are in the Department of Chemistry and Department of Biochemistry, Molecular Biology, and Cellular Biology, Northwestern University, Evanston, IL 60208, USA.

*To whom correspondence should be addressed.

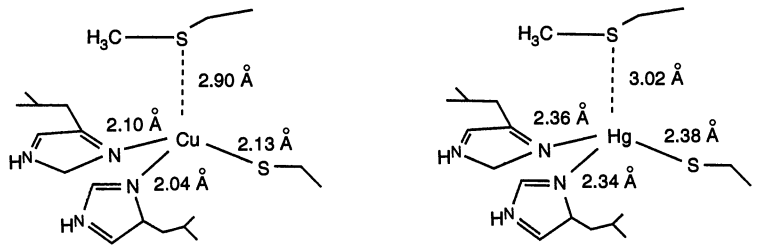

Scheme 1.

smaller complex, Hg-plastocyanin (*7*). Mercuric ion, when substituted into this 99–amino acid blue copper protein, adopts the coordination environment of the native metal ion, as shown by the absence of marked structural differences in x-ray crystal structures of the Hg(II)-substituted and native Cu(II) forms of the protein (see Scheme 1) (*25*).

The pulse sequence (*26*) $\pi/2_x(^1H)$-Δ-$\pi/2_\phi(^{199}Hg)$-$t_1/2$-$\pi_x(^1H)$-$t_1/2$-$\pi/2_x(^{199}Hg)$-Δ-Acq (^1H) (decouple ^{199}Hg) was used to obtain the 2D NMR spectra, where the delay (Δ) is normally set to $1/(2J)$ (J is the coupling constant). In the absence of appropriate J values for Hg-His and Hg-Met ligation, a series of preparation delays from 1.5 to 20 ms were examined (*27*) and two were sufficient for resolving signals from all of the established ligands to Hg(II): A 3-ms delay provided maximal signal for the larger Cys ^1H-^{199}Hg coupling, and 15 ms was optimal for the more weakly coupled His and Met protons.

The 2D proton-detected HMQC spectra of ^{199}Hg-plastocyanin (Fig. 1) yielded HMQ coherences over three and four bonds for two His, one Cys, and one Met ligand coordinated to the ^{199}Hg. Given the crystal structure of Hg-plastocyanin, the ^1H NMR resonances at 8.07, 7.98, and 7.33 ppm, were attributed to His ring protons of His^{46} and His^{117}. The ^1H NMR resonance observed at 3.01 ppm was assigned to Cys^{84} C_β-^1H, and while the 0.67 ppm resonance was assigned to Met^{92} C_ε-^1H. The small peak at 3.42 ppm could be attributed to either the second Cys^{84} C_β-^1H or to Met^{92} C_γ-^1H. Based on the optimal delays, the ^1H-^{199}Hg coupling constants for a C_β proton of the Cys ligand ($^3J_{H\text{-}Hg}$) can be as large as 160 Hz. Similarly, the $^3J_{H\text{-}Hg}$ or $^4J_{H\text{-}Hg}$ values for C_ε protons of Met or the δ- or ε-protons of His ligands can be as large as 30 Hz. Our estimated ^3J $^1H\beta$(Cys)-^{199}Hg values are consistent with those measured for the structurally characterized 6-kD protein, ^{199}Hg-rubredoxin (*2*). These latter values vary in a Karplus-type manner from 13 to 116 Hz and are the only other ^1H-^{199}Hg coupling constants reported for mercuric thiolate complexes or proteins.

$^1H\{^{199}Hg\}$ HMQC of carbonic anhydrase (CA). The MerR protein, a 32-kD dimer, binds a single Hg(II) and is approximately three times the size of plastocyanin. The HMQC transfer in the weakly coupled ^1H(His)-^{199}Hg spin system was tested with the Hg-substituted form of bovine CA. This 255–amino acid protein (29.5 kD) has a rotational correlation time comparable to that of the MerR dimer. Three His side chains bind a single Zn(II) ion in the native form of CA (*17*).

The preparation delays determined for ^{199}Hg-plastocyanin allowed acquisition of a high signal-to-noise ratio (S/N) $^1H\{^{199}Hg\}$ HMQC spectrum for the ^{199}Hg-substituted form of CA. The $^1H\{^{199}Hg\}$ HMQC spectrum (Fig. 2), with Δ = 15 ms, reveals five ^1H resonances at 8.88, 7.93, 7.52, 6.21, and 5.85 ppm corresponding to a −1270 ppm ^{199}Hg chemical shift ($\nu_{1/2}$ = 1050 Hz). This ^{199}Hg resonance, also measured by "direct observe" ^{199}Hg NMR, occurs 40 ppm downfield from the −1310 ppm resonance reported for human CA in the first direct observe study of a ^{199}Hg-protein complex (*6*). The ^1H resonances from three His ligands are clearly observed in Fig. 2, demonstrating that $^1H\{^{199}Hg\}$ HMQC experiments at this field strength allow detection of weakly coupled protons in a 29.5-kD protein.

$^1H\{^{199}Hg\}$ HMQC of the protein-DNA complex. The preparation delays established above allow acquisition of $^1H\{^{199}Hg\}$ HMQC spectra for both ^{199}Hg-MerR (31.6 kD) and the higher molecular weight DNA complex of ^{199}Hg-MerR. This complex was prepared with a 34-bp oligonucleotide that contains the complete MerR binding site (52.4 kD). In the Δ = 3 ms spectrum, two resolvable ^1H chemical shifts correlate with the −110 ppm ^{199}Hg resonance at 3.25 and 3.60 ppm, consistent with the coupling of C_β-^1H from Cys (Fig. 3). These same methylene ^1H chemical shifts were observed for ^{199}Hg-MerR in the absence of DNA, indicating that the Hg coordination environment does not change when the complex is bound to the DNA. The S/N of a proton slice through the ^{199}Hg resonance is ~13 for these Cys signals. There is no sign of any ^1H resonance arising from His or Met in the Δ = 15 ms spectrum for both ^{199}Hg-MerR and ^{199}Hg-MerR/DNA complex (Fig. 3).

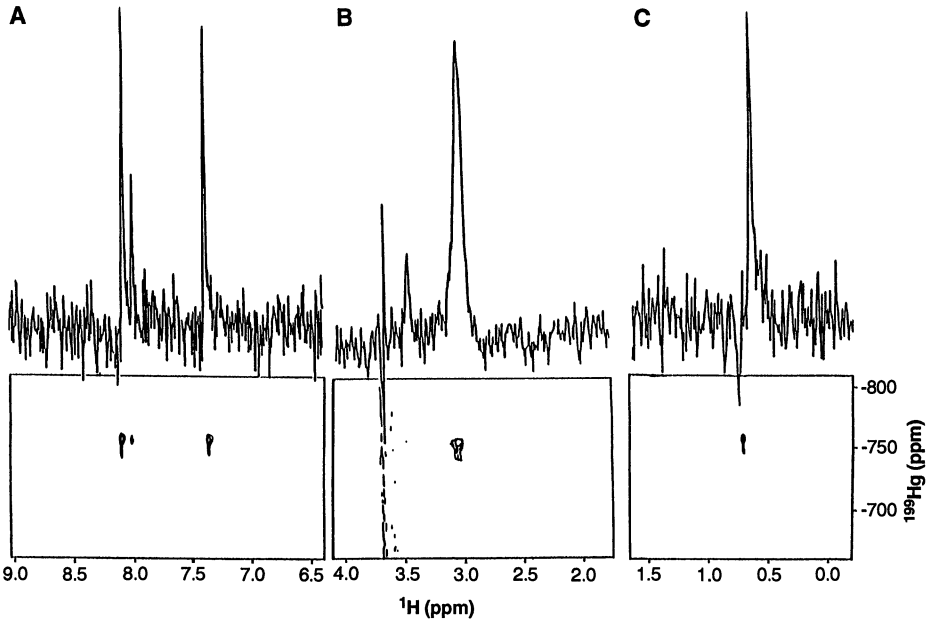

Fig. 1. Proton-detected heteronuclear $^1H\{^{199}Hg\}$ double-quantum coherence in Hg(II)-substituted spinach plastocyanin (*43*). All protein samples were prepared with 91% isotopically enriched ^{199}HgO obtained from Oak Ridge National Laboratory. The contour plots are of two-dimensional (2D) Fourier transform NMR spectra obtained as described in the text. ^1H slices are shown at the top of each spectral region displayed. Preparation delays were 15 ms for (**A**), 3 ms for (**B**), and 15 ms for (**C**). A spectral width of 7246 Hz for ^1H($F2$) and 32,221 Hz for ^{199}Hg ($F1$) were used. For each of 64 t_1 blocks that were accumulated, 512 transients were collected in $F2$. The ^1H 90° pulse used was 7.8 μs, and the $^{199}Hg(90°)^{-1}$ was 19 μs, as measured with $Hg(CH_3)_2$. Acquisition times were 12 hours total for the complete 2D spectrum at each delay. The residual HOD signal was selectively presaturated during the relaxation delay. The spectra were ^{199}Hg-decoupled with a GARP decoupling scheme.

Based on the observed S/N for the Cys protons in the Hg-MerR spectra, signals from His or Met should be observable under these experimental conditions if they are coordinated to the Hg(II) center. Given the Hg-CA results, it is unlikely that magnetization was lost in the transfer processes between ^{199}Hg and weakly coupled protons of coordinated His or Met side chains.

These 2D chemical shift correlation experiments indicate that Hg(II) is coordinated to Cys with little or no primary bonding to His or Met residues in either Hg-MerR or its complex with DNA. Because of overlap of methylene protons and variations in Karplus-type coupling (*2*), the number of Cys side chains is not readily obtained from these experiments. Additional structural information is available in the ^{199}Hg chemical shift if structure-shielding correlations can be established for coordination environments characteristic of biological systems.

^{199}Hg-MerR chemical shift. Insights into the metal ion receptor site are obtained by comparing the ^{199}Hg-MerR chemical shift to those of structurally characterized model complexes and metalloproteins. In spite of large CSA contributions, ^{199}Hg-resonances are readily obtained for proteins by direct methods as well as by indirect detection in the 2D experiments described above. In fact, the two methods complement each other. Relatively fast ^{199}Hg longitudinal relaxation times (T_1) allow the use of 90° pulse widths that lead to the acquisition of good S/N ^{199}Hg spectra for relatively large spectral windows in a few hours with small quantities of protein (10 to 40 mg) (*7*). Thus the ^{199}Hg chemical shift is most efficiently obtained from the 1D experiment. This determination then allows a smaller window for the ^{199}Hg dimension in ^{1}H{^{199}Hg} HMQC experiment, decreasing the total accumulation time.

Direct observe ^{199}Hg spectra (Fig. 4) reveal ^{199}Hg chemical shifts of −106 and −109 ppm for Hg-MerR and its complex with DNA, respectively. These ^{199}Hg linewidths are not unexpected given the relatively large size of the MerR dimer (32 kD) and the MerR-DNA complex (52 kD). These chemical shifts fall within the −80 to −160 ppm range (Fig. 5) established for structurally characterized three-coordinate mercuric complexes of aliphatic thiolates and significantly differ from the −300 to −500 ppm (*5*, *28*) range of solution shifts reported for aliphatic $Hg(SR)_4^{2-}$ complexes (R is generally an alkyl or aromatic group).

The most definitive correlations between structure and chemical shift are obtained from solid state ^{199}Hg NMR studies of crystallographically characterized Hg(II) model compounds. Small Hg(II) complexes can undergo dissociation or oligomerization reactions in solution NMR experiments. These relations are better established for $Hg(SR)_3$, complexes than for $Hg(SR)_4$ analogs: Little solid state data are available for the latter, and complexes are typically generated in situ with no corroboration of structure. Some solid state data are available for both Hg(II) complexes of alkyl (*5*, *29*) and aromatic thiolate complexes (*4*, *29*). Although the isotropic chemical shifts of the latter provide insights into trends, inductive effects of the aromatic ring can lead to significant shielding, in some cases amounting to 200 ppm (*5*), which make them less useful as guides to Hg-Cys coordination in proteins. Recently, solution ^{199}Hg chemical shifts of crystallographically characterized four-coordinate Hg compounds of an aliphatic thiolate were reported to be −126 and −134 ppm (*30*). These solution shifts are outside the range of the four-coordinate complexes described above but within that established for aliphatic three-coordinate complexes. Until solid state chemical shifts are reported, the species giving rise to these two solution chemical shifts remain in question. For instance, partial dissociation of the chelating dithiol ligand in solution or severe distortion of the primary coordination sphere from T_d geometry could lead to deshielding. Further insights into the $Hg(SR)_4^{2-}$ chemical shift range can be obtained from NMR studies of structurally characterized Hg-substituted metalloproteins.

Benchmark ^{199}Hg-protein chemical shifts. The ^{199}Hg-substituted form of the zinc finger protein GAL4(1-65) serves as a structural model for one type of four-coordinate Hg(II) thiolate center. The 3D structure of the Zn(II) and Cd(II) complexes of GAL4(1-65) DNA binding domain, determined by x-ray crystallography and NMR spectroscopy (*31*–*33*), reveal a binuclear center with two bridging and two terminal Cys ligands per metal. Because the Hg_2- and Zn_2-GAL4 complexes are isostructural (*31*), the peptide tertiary structure remains essentially unchanged when the larger Hg(II) ion is substituted for Zn(II). The solution ^{199}Hg NMR spectrum of $^{199}Hg_2$GAL4(1-65) (Fig. 4C) exhibits two resonances of the same intensity at −243

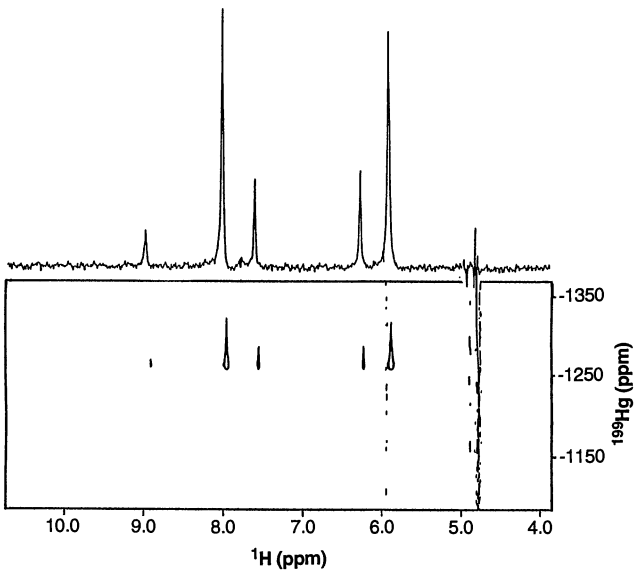

Fig. 2. The ^{1}H{^{199}Hg} HMQC spectrum of ^{199}Hg-CA (*44*) was obtained on the Bruker 600 as described for Fig. 1. A preparation delay Δ = 15 ms and spectral widths of 7246 Hz for ^{1}H(*F2*), and 32,207 Hz for ^{199}Hg (*F1*) were used. The spectra were collected at 20°C, and the data set was processed by using line broadening (5 Hz in the *F1* dimension and 200 Hz in the *F2* dimension).

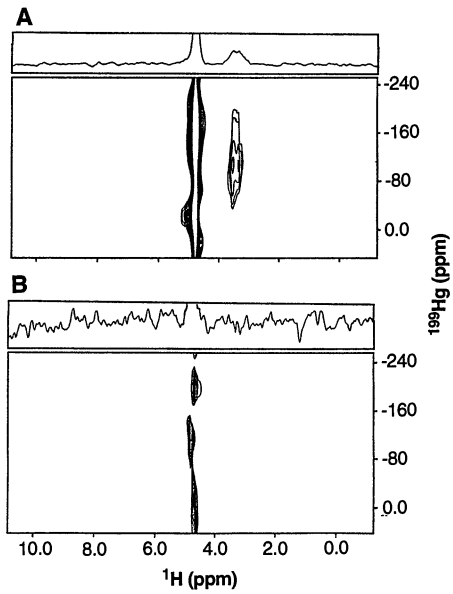

Fig. 3. ^{1}H{^{199}Hg} HMQC spectra of a Hg-MerR–DNA complex. The spectra were acquired on Hg-MerR/DNA sample (*45*) and displayed as described in Fig. 1. Preparation delays Δ were 3 ms for (**A**) and 15 ms for (**B**). Spectral widths of 7246 Hz for ^{1}H(*F2*) and 32,243.8 Hz for ^{199}Hg(*F1*) were used. For each of 64 t_1 blocks that were accumulated, 1440 transients for (A) and 1800 transients for (B) were collected in *F2*. Total acquisition times were (A) 35 and (B) 48 hours. Both data sets were processed by using line broadening (15 Hz in the *F1* dimension and 500 Hz in the *F2* dimension). The spectra were collected at 25°C.

and −308 ppm relative to neat $Hg(CH_3)_2$ and provide a benchmark for shielding in a thiolate-bridged binuclear $^{199}Hg(II)$ site. In the ^{113}Cd NMR spectra of $Cd_2GAL4(1-63)$, two resonances are separated by only 37 ppm (*21*), as expected for the narrower range of ^{113}Cd chemical shifts. Another calibration of ^{199}Hg chemical shift for a $Hg(S\text{-}Cys)_4$ environment is provided from the electron-transfer protein rubredoxin. A ^{199}Hg chemical shift at −241 ppm, determined for this protein by indirect detection, was assigned to a four-coordinate mercuric thiolate center (*2*). These three ^{199}Hg chemical shifts of structurally characterized Hg-protein complexes define a range for distorted tetrahedral Hg(II) centers coordinated to four Cys thiolates that is well separated from that of $Hg(SR)_3$. The resonance observed for MerR clearly does not fall within this $Hg(SR)_4$ range.

Several other coordination environments for Hg-MerR can likewise be ruled out. For example, the ^{199}Hg-MerR chemical shift is well outside the values observed when one or two thiolates are joined by more shielding ligands, such as a thioether sulfur of Met or an imidazole nitrogen of His. The ^{199}Hg chemical shift for the structurally characterized, Hg-substituted form of plastocyanin at −749 ppm (*7*) corresponds to a $Hg(N\text{-}His)_2(S\text{-}Cys)(S\text{-}Met)$ environment. Recently, ^{199}Hg NMR spectra of the Hg-substituted LIM domain protein CRIP (*34*) have been obtained (*35*). Two ^{199}Hg chemical shifts of −243 and −383 ppm were observed and are consistent with $Hg(S\text{-}Cys)_4$ and $Hg(S\text{-}Cys)_3(N\text{-}His)$ environments, respectively (*35*). Although ^{199}Hg chemical shifts have not been reported for other possible environments, including $Hg(Cys)_3(S\text{-}Met)$ centers, such four-coordinate complexes are expected to be more shielded than ^{199}Hg-MerR. If we consider the HMQC results described above, such coordination is unlikely.

A trigonal $Hg(S\text{-}Cys)_3$ receptor complex. Relative to the ^{199}Hg chemical shifts established for biologically relevant complexes (Fig. 5), Hg-MerR falls in the middle of a distinct group of trigonal-thiolate complexes. These planar, three-coordinate complexes of aliphatic thiolates are the most deshielded mercuric-thiolate, -amine, or -carboxalato complexes studied to date. We propose that molecular recognition at the metal site in the activated receptor complex involves a mercuric ion coordinated to only three Cys side chains in a trigonal planar environment as shown below. An alternative that we cannot rule out at this time is a pyramidal, three-coordinate environment; however, the chemical shift of such a species is expect to be outside of the −80 to −160 ppm range characteristic of the planar models.

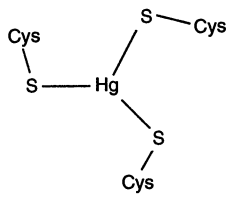

This Hg(II) configuration in the receptor-DNA complex provides structural insights into the metal ion sensitivity and selectivity of MerR.

The reaction of nanomolar Hg(II) with the receptor in the presence of excess thiol buffered at pH 7 is shown in Eq. 1. Under these conditions, the predominate form of Hg(II) in the buffer is the two-coordinate thiolate complex.

$$Hg(SR)_2 + MerR \rightarrow Hg\text{-}MerR + 2RSH \quad (1)$$

The driving force for tight binding of Hg(II) by MerR apparently includes favorable entropic terms arising from the chelate effect at this tridentate site and favorable enthalpic factors arising from formation of a third metal-thiolate bond. Given the thermodynamics of Hg-thiolate interactions, this enthalpic contribution of the third Hg-SR bond in the Hg-MerR complex can be stabilizing by as much as ~8 kcal/mol if the protein excludes protons or water from the metal-receptor site (*5*).

These structural insights also provide a basis for understanding the receptor's pronounced selectivity for Hg(II). In the Fe, Cu, and Zn proteins discussed above, the native metal ion adopts a four- or five-coordinate geometry. The Hg(II) receptor site in MerR, however, adopts a three-coordinate geometry that is uncommon for most competing metal ions. Thus, the coordination chemistry preferences of both Hg(II) and the competing metal ion must be taken into account to understand the basis of MerR's selectivity for Hg(II). For example, when Zn(II) is the competing metal, it may form a trigonal thiolate complex or it may adopt higher coordination numbers by conscripting other sidechains as ligands.

Although mercuric ion has the propensity to form complexes with low coordination numbers, it can bind additional ligands if the coordination environment is mandated by the conformation of a relatively rigid chelation site in a protein. The best example of this phenomenon is seen in the series of crystallographic and NMR structures of the blue copper proteins where, in the presence or absence of a range of metal ions, the configuration of the ligands or the local geometry at the metal center remains relatively constant (*25*, *36*, *37*). MerR may impose a rigid coordination environment on all metals in a similar manner.

On the other hand, the coordination number and geometry at the metal may not be restricted by the tertiary structure of the receptor. In this scenario, MerR may exhibit conformational flexibility in metal binding. Selectivity in this case arises only if a few of the resulting metal-induced MerR conformations are competent to activate transcription. Resolution of these mechanisms for metal ion discrimination will require determination of the coordination environment in MerR complexes with other metal ions.

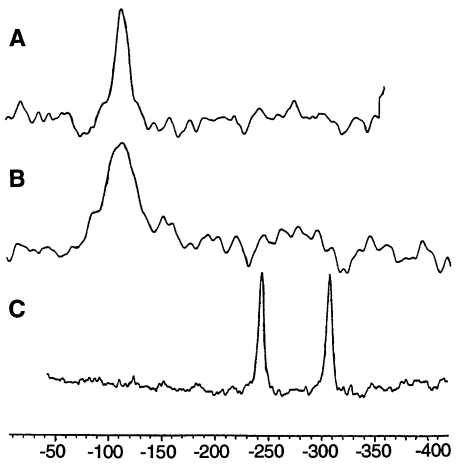

Fig. 4. ^{199}Hg NMR spectra at 107.43 MHz of (**A**) ^{199}Hg-MerR (*46*) (**B**) ^{199}Hg-MerR–DNA (*45*), and (**C**) $^{199}Hg_2GAL4(1-65)$ (*47*). These spectra were obtained with a Bruker 600 spectrometer (14.09 T, 107.4 MHz for ^{199}Hg) equipped with a 5-mm broadband tunable probe. The 90° ^{199}Hg pulse was 10.6 μs. Spectrum (A) was collected in 46 hours with 770,273 scans, a pulse angle of 80°, a sweep width of 71,428 Hz, an acquisition time of 115 ms, and a relaxation delay of 0.1 s. The data were processed by applying a 700-Hz line broadening prior to Fourier transformation. The single peak has a S/N of 11 with $\nu_{1/2}$ = 1700 Hz. Spectrum (B) was collected in 63 hours with 1,142,717 scans, a pulse angle of 90°, a sweep width of 83,333 Hz, an acquisition time of 98 ms, and a relaxation delay of 0.1 s. The data were processed by applying an 800-Hz line broadening prior to Fourier transformation. The single resonance has a S/N of 9 with a $\nu_{1/2}$ = 3600 Hz. Both MerR spectra were collected at 30°C. At this field strength, ^{199}Hg relaxation rates for these complexes are likely to be shorter than the ~10-ms T_1 and ~0.1-ms T_2* values reported for smaller ^{199}Hg-substituted proteins, such as plastocyanin (10.5 kD) (*7*). Spectrum (C) for GAL4 was collected in 4 hours with 70,000 scans, a pulse angle of 90°, a sweep width of 71,428 Hz, an acquisition time of 115 ms, and a relaxation delay of 0.1 s. The data were processed by applying a 200-Hz line broadening prior to Fourier transformation. Both peaks have a S/N of 22 with $\nu_{1/2}$ = 500 Hz and were collected at 20°C. All spectra were collected without proton decoupling because the ^{199}Hg NMR line shape or line widths for smaller Hg(II)-protein complexes are unchanged upon decoupling (*7*). Chemical shifts are relative to neat $(CH_3)_2Hg$ at 25°C.

Allostery of metal and DNA binding to the receptor. We have shown that allosteric signaling by MerR requires the metal-receptor complex to change the local structure of the promoter (*10, 11*), but does DNA binding to its receptor site lead to a structural change in the metal-receptor site? The ^{199}Hg chemical shift of Hg-MerR and the ^{199}Hg-coupled ^{1}H chemical shifts of coordinated Cys protons do not change within experimental error upon protein-DNA complex formation. We conclude that the Hg(II) coordination environment is not allosterically modulated by DNA binding to the receptor: No significant difference in the number, geometry, or types of primary ligands to the Hg(II) exist between the two states.

The driving force for conformational changes in DNA induced by Hg-MerR come in part at the expense of the DNA-protein binding free energy (*8*) and from the coordination of Hg(II) to a single high-affinity site in MerR. Hg-MerR binds less tightly to DNA than apo-MerR by ~0.5 kcal/mol, and as expected for a thermodynamic cycle, the affinity of Hg(II) for the MerR-DNA complex drops by a reciprocal amount (*38*). Given the negligible effect of DNA binding to MerR on the Hg(II) coordination environment, we conclude that the structural changes in this allosteric system are vectorial: Hg(II) coordination in the trigonal receptor site drives the protein, and thus the bound DNA, into a new conformation, but binding of DNA to MerR does not lead to an alteration in the primary Hg(II) coordination environment. The energetic linkage described above must be accounted for by changes in conformation at other sites in the protein-DNA complex. The allosteric effector, Hg(II), thus binds to its receptor site in the same geometry whether or not MerR is bound to its regulatory target, the *mer* operator.

^{199}Hg spectroscopy as a probe of coordination environments in other metalloproteins. We have resolved four fundamental and sometimes controversial issues concerning application of ^{199}Hg NMR methods to biopolymers and conclude that such methods will be useful in an array of problems in structural biology and inorganic biochemistry. Contrary to previous speculation (*4*), ^{199}Hg spectra with reasonable line widths can be obtained in direct-observe experiments on three-coordinate Hg(II) centers in large proteins. Second, the coupling of ^{199}Hg to side chain ^{1}H-spin systems can be used in high-field experiments on relatively large proteins, at least up to the 50-kD range, even in experiments at high field strength where CSA effects are likely to dominate relaxation processes and relaxation rates are expected to be rapid. In the absence of additional details on relaxation mechanisms in each of the coordination environments, it is difficult to specify the optimal field strength for ^{199}Hg-protein experiments. We have also shown that the isotropic chemical shift reflects the geometry, the number, and the type of ligating side chains in the limited number of model complexes and ^{199}Hg-substituted proteins characterized to date, and we have established a preliminary map of the shielding trends for these Hg(II) environments. As noted previously, the sometimes competing effects of the geometry, ligand type, and coordination number can influence the ^{199}Hg chemical shift tensor (*4, 5, 29*) and must be considered before extrapolation of the shielding trends described here. Additional data on characterized model compounds and proteins are desirable in this regard. Finally, these results underscore other observations that Hg(II) can readily displace and subsequently adopt the coordination environment of the native metal in several types of Fe, Cu, and Zn metalloproteins. Thus, we anticipate that direct observe– and 2D ^{199}Hg–based methods will be useful structural probes of Fe, Cu, and Zn transcription factors or metalloproteins of moderate size.

Since its introduction as a biological probe by Armitage, Coleman, and co-workers in 1976 (*39*), ^{113}Cd NMR methods have been valuable tools in the characterization of metal-binding sites and structures of a variety of proteins (*40, 41*). The ^{199}Hg NMR methods described here provide an alternative to, and in some cases advantages over, the well-established ^{113}Cd-based methods. For instance, the large chemical shift dispersion for ^{199}Hg allows clear differentiation between a variety of $M(SR)_n$ environments. In comparison, the coordination environments of CdS_3 and CdS_4 complexes are difficult to assign based on the solution or isotropic ^{113}Cd chemical shifts of the available model complexes (*4*). Also, the short relaxation times for ^{199}Hg complexes allow for a rapid rate of data accu-

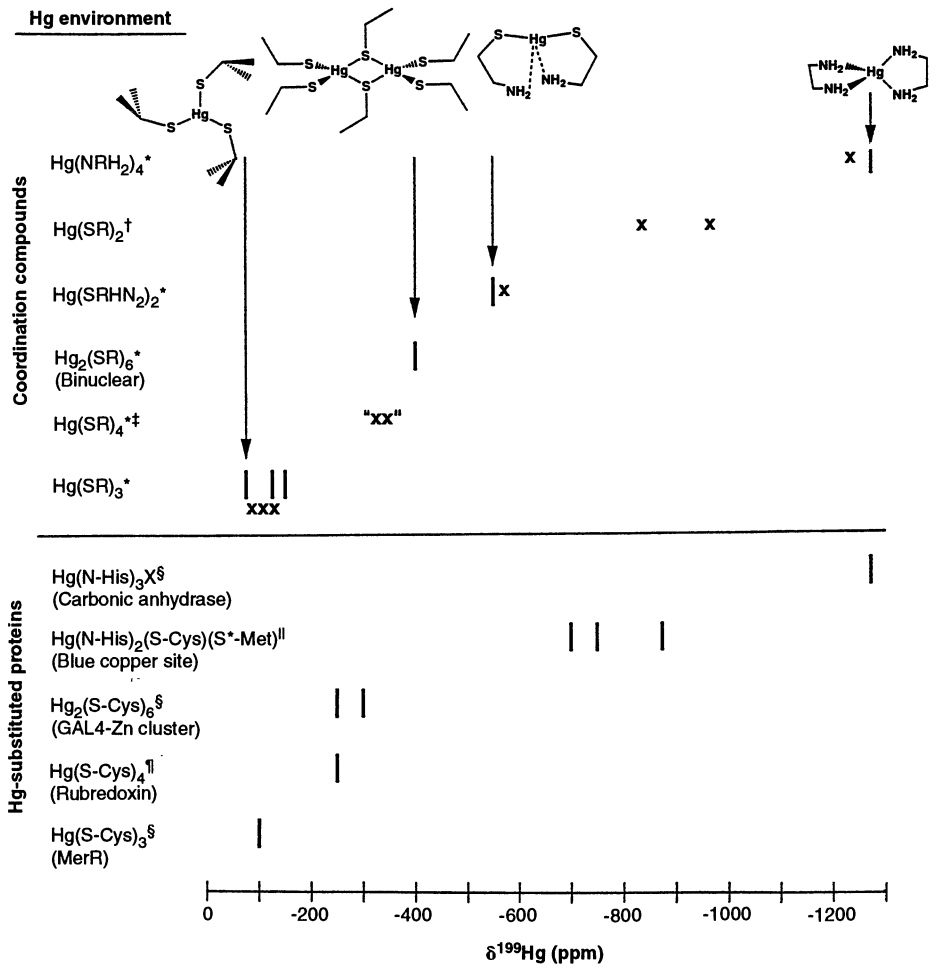

Fig. 5. ^{199}Hg chemical shifts of aliphatic amine/thiol model complexes and ^{199}Hg-substituted proteins. The solution shifts (x, "x" generated in situ) and isotropic solid state (I) ^{199}Hg shifts are for model complexes with various coordination environments, where NRH_2 represents a primary amine and SR represents a thiolate. The coordination environments of the Hg proteins (where solution chemical shifts = I) include His imidazole N-His, Cys thiolate S-Cys, and Met thioether S*-Met ligands. For futher information, see the following references: * (*5, 28*); † (*48*); ‡ (*49*); § [this work and (*7*); || (*50*); and ¶ (*2*).

mulation in direct-observe experiments (*7*). Intriguingly, T_2 relaxation processes for the various ^{199}Hg-proteins studied to date are not so fast as to allow significant spin-diffusion in the magnetization transfer experiments. Apparently, a favorable combination of rapid relaxation rates at high field strength and large ^{1}H-^{199}Hg coupling constants allow application of the coherence transfer methods to metalloproteins fivefold larger than those reported in ^{1}H{^{113}Cd} HMQC experiments. Finally, Hg(II) is readily exchanged for the native metal in many Cu, Zn, and Fe metalloproteins (*42*). These attributes suggest that ^{199}Hg NMR methods can play a wider role in structural, spectroscopic, and chemical studies of metal binding domains in biopolymers where the tertiary structure of the folded polymer dictates the coordination geometry of the metal ion.

REFERENCES AND NOTES

1. K. H. Falchuk, L. J. Goldwater, B. L. Vallee, in *The Chemistry of Mercury*, C. A. McAuliffe, Ed. (Macmillan, Toronto, 1977), pp. 260–277; I. Bertini, C. Luchinat, in *Bioinorganic Chemistry*, I. Bertini *et al.*, Eds. (University Science Books, Mill Valley, CA, 1994), pp. 43–48.
2. P. R. Blake *et al.*, *New. J. Chem.* **18**, 387 (1994).
3. B. Wrackmeyer and R. Contreras, *Annu. Rep. NMR Spectrosc.* **124**, 267 (1992).
4. R. A. Santos, E. S. Gruff, S. A. Koch, G. S. Harbison, *J. Am. Chem. Soc.* **113**, 469 (1991).
5. J. G. Wright, M. J. Natan, F. M. MacDonnell, D. M. Ralston, T. V. O'Halloran, in *Progress in Inorganic Chemistry*, S. J. Lippard, Ed. (Wiley, New York, 1990), vol. 38, pp. 323–412.
6. J. L. Sudmeier and T. G. Perkins, *J. Am. Chem. Soc.* **99**, 7732 (1977).
7. L. M. Utschig, J. G. Wright, G. Dieckmann, V. Pecoraro, T. V. O'Halloran, *Inorg. Chem.*, in press.
8. T. V. O'Halloran, B. Frantz, M. K. Shin, D. M. Ralston, J. G. Wright, *Cell* **56**, 119 (1989).
9. D. M. Ralston and T. V. O'Halloran, *Proc. Natl. Acad. Sci. U.S.A.* **87**, 3846 (1990).
10. B. Frantz and T. V. O'Halloran, *Biochemistry* **29**, 4747 (1990).
11. J. E. Bradner, T. V. O'Halloran, *Nature* **374**, 371 (1995).
12. S. P. Watton *et al.*, *J. Am. Chem. Soc.* **112**, 2824 (1990).
13. J. G. Wright, H.-T. Tsang, J. E. Penner-Hahn, T. V. O'Halloran, *ibid.*, p. 2434.
14. J. D. Helmann, D. T. Ballard, C. T. Walsh, *Science* **247**, 946 (1990).
15. W. Ross, S.-J. Park, A. O. Summers, *J. Bacteriol.* **171**, 4009 (1989).
16. T. V. O'Halloran, *Science* **261**, 715 (1993).
17. S. J. Lippard and J. M. Berg, *Principles of Bioinorganic Chemistry* (University Science, Mill Valley, CA, 1994).
18. J. W. R. Schwabe and A. Klug, *Nature Struct. Biol.* **1**, 345 (1994).
19. J. D. Otvos, H. R. Engeseth, S. Wehrli, *J. Magn. Reson.* **61**, 579 (1985).
20. M. H. Frey *et al.*, *J. Am. Chem. Soc.* **107**, 6847 (1985).
21. T. Pan and J. E. Coleman, *Proc. Natl. Acad. Sci. U.S.A.* **87**, 2077 (1990).
22. D. H. Live, C. L. Kojiro, D. Cowburn, J. L. Markley, *J. Am. Chem. Soc.* **107**, 3043 (1985).
23. J. E. Coleman, *Methods Enzymol.* **227**, 16 (1993).
24. The ^{113}Cd-plastocyanin (0.5 Cd atoms per protein) and ^{113}Cd-MerR (0.9 Cd atoms per dimer) samples were prepared by similar methods as their ^{199}Hg-derivatives detailed below. Optimum delays on the Bruker 600 (14.09T, 133.1 MHz for ^{113}Cd) equipped with a 5-mm broadband tunable probe were determined for the ^{113}Cd-plastocyanin [^{113}Cd (90°) = 13 μs and delay Δ = 10 ms and 50 ms] and ^{1}H resonances from two His, one Met, and one Cys ligands were observed as previously reported (*22*). Numerous attempts to observe a ^{1}H{^{113}Cd} HMQC spectrum of ^{113}Cd-MerR with the parameters optimized for ^{113}Cd-plastocyanin were unsuccessful.
25. W. B. Church, J. M. Guss, J. J. Potter, H. C. Freeman, *J. Biol. Chem.* **261**, 234 (1986).
26. A. Bax, R. H. Griffey, B. L. Hawkins, *J. Magn. Reson.* **55**, 301 (1983); in this sequence, ϕ is phase cycle, t_1 is an incremented delay, and Acq is acquire.
27. At the initiation of these studies, we found no relevant ^{1}H-^{199}Hg coupling constants (*J*) reported, so initial 1/(2*J*) values were estimated. The delay Δ was optimized by comparing the signal-to-noise of the transformed ^{1}H spectrum of the first *F2* t_1 block obtained from a series of time delays.
28. J. W. Bryson, S. P. Watton, T. V. O'Halloran, in preparation.
29. M. J. Natan, C. F. Millikan, J. G. Wright, T. V. O'Halloran, *J. Am. Chem. Soc.* **112**, 3255 (1990).
30. N. Govindaswamy, J. Moy, M. Millar, S. A. Koch, *Inorg. Chem.* **31**, 5343 (1992).
31. R. Marmorstein, M. Carey, M. Ptashne, S. C. Harrison, *Nature* **356**, 408 (1992).
32. P. J. Kraulis, A. R. C. Raine, P. C. Gadhavi, E. D. Laue, *ibid.*, p. 448.
33. J. D. Baleja, R. Marmorstein, S. C. Harrison, G. Wagner, *ibid.*, p. 450.
34. J. L. Kosa *et al.*, *Biochemistry* **33**, 468 (1994).
35. L. M. Utschig and T. V. O'Halloran, in preparation.
36. J. M. Moore *et al.*, *J. Mol. Biol.* **221**, 533 (1991).
37. T. P. J. Garrett, D. J. Clingeletter, J. M. Guss, S. J. Roger, H. C. Freeman, *J. Biol. Chem.* **259**, 2822 (1984).
38. J. Parkhill, A. Z. Ansari, J. Wright, N. L. Brown, T. V. O'Halloran, *EMBO J.* **12**, 413 (1993).
39. I. M. Armitage, R. T. Pajer, A. J. M. Schoot Uiterkamp, J. F. Chlebowski, J. E. Coleman, *J. Am. Chem. Soc.* **98**, 5710 (1976).
40. P. D. Ellis, *Science* **221**, 1141 (1983).
41. M. F. Summers, *Coord. Chem. Rev.* **86**, 43 (1988).
42. L. M. Utschig, J. G. Wright, T. V. O'Halloran, in *Methods Enzymol.* **226**, 71 (1993).
43. Three equivalents (eq) of the ^{199}Hg(II) were added to apo-plastocyanin and the metal protein solution was stirred for 2 hours. Free-metal ions were separated from the Hg-protein complex by gel filtration on a Sephadex G25 column with a 25 mM tris-Cl buffer, pH 8.0. Inductively coupled plasma–atomic emission spectroscopy (ICP-AES) on the subsequent protein fractions was used to determine the amount of Hg(II) bound to the protein. The protein sample was concentrated to a final NMR sample volume of 0.4 ml by using a Centriprep-3 device and was exchanged into a 95% (v/v) D_2O 80 mM sodium phosphate buffer, pH 7.0. The final concentration of this sample was 1.6 mM ^{199}Hg-plastocyanin, with a metal-to-protein ratio of 0.8.
44. Bovine CA II was purchased from Sigma. The native zinc metal was removed by dialysis against 75 mM pyridine-2,6-dicarboxylic acid, pH 7.0. The apo-protein was then dialyzed into a 50 mM tris-acetate, pH 8.0 buffer. The Hg(II) derivative of the protein was prepared by addition of 3 eq of ^{199}Hg(II) with stirring under N_2 for 3 hours. Unbound metal ion was removed by size-exclusion chromatography on a Sephadex G-25 column. The protein was analyzed for Hg content by ICP-AES. The protein content was estimated by using an extinction coefficient $\varepsilon_{280} = 57{,}000\ M^{-1}\ cm^{-1}$, which indicated a fraction of 0.5 Hg atoms bound per protein molecule. The sample was concentrated by using Centriprep-10 filtration devices and exchanged into 96% D_2O, 50 mM tris-acetate, pH 8.0. The final concentration of this sample was 2.5 mM ^{199}Hg-CA.
45. Purified 34-nucleotide oligos containing the MerR binding site were purchased from Oligo's etc. The oligo, 5′-TGC TTG ACT CCG TAC ATG AGT ACG GAA GTA AGG T-3′, was hybridized to its complimentary strand. Previous experiments have shown that MerR binds with high affinity to DNA with 30 or more base pairs that contain the above sequence (*38*). Precipitated ^{199}Hg-MerR, prepared as described below, was resuspended with the hybridized DNA, and the protein-DNA complexes were dialyzed extensively to remove any residual ammonium sulfate. The solution was concentrated to a final volume of 380 μl and a final concentration of 1.1 mM ^{199}Hg-MerR (1.1 Hg-to-dimer ratio), 0.95 mM double-stranded (ds) DNA (~0.4 μmol each DNA and MerR dimer) for the 1D ^{199}Hg NMR experiment and a final concentration of 1.0 mM ^{199}Hg-MerR (1.1 Hg-to-dimer ratio) and 0.9 mM ds DNA for the HMQC experiment. Both solutions contained 20 mM MES, 0.1 M NaCl, and 10 mM 2-mercaptoethanol (β-ME), pH 6.02 in >95% (v/v) D_2O.
46. MerR was purified as previously described [see (*8*) and J. G. Wright, thesis, Northwestern University (1991).] The Hg(II) derivative of the protein was prepared by addition of 1.6 eq of ^{199}Hg(II) to 20 mg of apo-MerR in a buffer system containing 1 mM β-ME. The protein was gel filtered through a Sephadex G-25 Fine (Pharmacia) column to remove any excess metal. The protein fractions were ammonium sulfate precipitated and resuspended in 700 μl of 20 mM MES, 0.2 M NaCl, and 1 mM β-ME, pH 6.02, 95% (v/v) D_2O to a final concentration of 580 μM Hg-MerR dimer. Analysis of an aliquot of the solution by BioRad Assay ($\varepsilon_{280\ nm}$ for MerR monomer is $5.8 \times 10^3\ M^{-1}\ cm^{-1}$) and ICP-AES established that 1.1 Hg(II) was bound per dimer of MerR.
47. The plasmid pTac-GAL4(1-65) for the expression of the amino-terminal 65–amino acid fragment of GAL4 was generously donated by R. Marmorstein and S. Harrison. Zn_2GAL4(1-65) was purified by cation exchange and gel filtration chromatography as described elsewhere [see J. W. Bryson, thesis, Northwestern University (1994)]. Purified GAL4(1-65) was dialyzed against 50 mM sodium phosphate, 150 mM sodium acetate, pH 6.5, 1 mM β-ME, and 1 mM EDTA. The protein was then incubated with 6 eq of ^{199}Hg(II) and gel filtered through a Sephadex G25 column. To remove residual zinc, this sample was then equilibrated with a 200 mM sodium phosphate, pH 5.0, 5 mM 2-mercaptoethanol, and 1.5 additional eq of ^{199}Hg(II). A second gel filtration step was then used to exchange the protein into the initial buffer. The protein was concentrated to a final volume of 500 μl and a final concentration of 3.4 mM $^{199}Hg_2$Gal4 in 150 mM sodium phosphate, 10 mM β-ME, pH 7.4, in 95% (v/v) D_2O.
48. M. M. Kubicki *et al.*, *J. Organomet. Chem.* **219**, 329 (1981).
49. G. K. Carson and P. A. W. Dean, *Inorg. Chim. Acta* **66**, 157 (1982).
50. L. M. Utschig, T. Baynard, C. Strong, T. V. O'Halloran, in preparation.

51. This research was supported by Dreyfus Teacher-Scholar Award, NIH (GM-38784 and GM-45972) to T.V.O., a NIH training grant (GM-08061) fellowship for L.M.U., and a Howard Hughes Medical Institute Predoctoral Fellowship for J.W.B. We thank D. Kushland, G. Ashley, and D. LeMaster for helpful discussions and R. Marmorstein, S. Harrison, B. Antonio, V. Pecararo, and G. Dieckmann for providing protein samples or plasmids. The 600 MHz Nuclear Magnetic Resonance Facility at Northwestern University is funded by the W. M. Keck Foundation (grant 891040), NIH (grant S10 RR05880), National Science Foundation (grant 8908093), State of Illinois Technology Challenge Grant Program (grant 90-82115), and Northwestern University.

23 December 1994; accepted 23 March 1995